GEORG-AUGUST-UNIVERSITÄT GÖTTINGEN

Fakultät für Physik

Spezialisierungspraktikum: Echodynamik mit statistischen Fluktuationen

Lab course: echo dynamics with statistical fluctuations

prepared by

Eric Bertok

from Kassel

at the Institut für Theoretische Physik

Thesis period:	19th April 2016 until 1st June 2016
Supervisor:	Markus Schmitt
First Rreferee:	Prof. Dr. Kehrein
Second referee:	Prof. Dr. Kree

Contents

1 Lab course

1.1 Theoretical foundation and numerical methods

1.1.1 Introduction, exact diagonalization

In what follows, we are interested in a one-dimensional XXZ Heisenberg chain with next-nearest neighbour coupling. As such, we consider the following Hamiltonian:

$$H(J,\mu) = H_1(J,\mu) + \lambda H_2(J,\mu), \tag{1.1}$$

$$H_n(J,\mu) = J\sum_{i=1}^{N}\left[\frac{1}{2}\left(S_i^+ S_{i+n}^- + S_i^- S_{i+n}^+\right) + \mu S_i^z S_{i+n}^z\right], \tag{1.2}$$

where the spins are labeled $i = 1,\ldots,N$ and J is the interaction constant. The scalar product for the spin operators $\mathbf{S}_i \cdot \mathbf{S}_{i+n}$ has been decomposed into creation-annihilation operators $S^{\pm} = S^x \pm iS^y$ while μ introduces an anisotropy for the z-direction compared to the x and y directions. Finally, λ is a parameter controlling the strength of the next-nearest neighbor (NNN) interactions cf. [1, p. 4ff.].
First, we would like to numerically compute the time evolution of such a system by means of exact diagonalization.

1.1.2 Block diagonalization

In the following section, we follow closely the techniques and notation from [7, p. 55ff.]. The states are denoted as $|S_0^z, S_1^z, \ldots, S_{N-1}\rangle$, where the subscript $i = 0,\ldots,N-1$ refers to the site i of our one-dimensional chain. A particular state is abridgedly labeled by arrows, e.g. $|\uparrow\downarrow\uparrow\downarrow\ldots\rangle$. Furthermore, periodic boundary conditions, which add additional symmetries, are assumed ($i = N-1+n \equiv n-1$). Exact diagonalization allows for total knowledge of the properties of a finite system by choosing a basis, setting up a Hamiltonian and diagonalizing it numerically. While theoretically applicable to any system size, this method is limited to around 30 spins, as

the computational cost for diagonalization is $\mathcal{O}(d^3)$ and the spin basis dimension d above grows like 2^N without utilizing symmetries. Symmetries can be used to transform the Hamiltonian matrix into block-diagonal form cf. [7, p. 56] with each block belonging to states with a conserved quantum number, thereby reducing the basis dimension. In this first chapter, only the conservation of z-component of the total spin ($\hat{=}$ total magnetization) $m_z = \sum_{i=0}^{N-1} S_i^z$ is used:
It is easy to verify, using the usual commutation relations for the spin operators that

$$[S_i^z, H] = \frac{1}{2}(A_1 + A_2), \tag{1.3}$$

$$A_n = S_i^+ S_{i+n}^- - S_i^- S_{i+n}^+ - S_{i-n}^+ S_i^- + S_{i-n}^- S_i^+. \tag{1.4}$$

By using the periodic boundary conditions it follows that

$$\sum_{i=0}^{N-1} A_n = \sum_{i=0}^{N-1} \left(S_i^+ S_{i+n}^- - S_i^- S_{i+n}^+ \right) - \underbrace{\sum_{i=n}^{N-1+n}}_{\equiv \sum_{i=0}^{N-1}} \left(S_i^+ S_{i+n}^- - S_i^- S_{i+n}^+ \right) = 0, \tag{1.5}$$

and therefore

$$[H, m_z] = 0, \tag{1.6}$$

meaning that m_z is a conserved quantity. By constructing a basis with fixed magnetization, blocks of size $M \times M$ with the same m_z can be considered independently. M is the fixed magnetization basis dimension: [7, 60]

$$M = \frac{N!}{n_\uparrow!\; n_\downarrow!}. \tag{1.7}$$

1.1.3 Bit representation

As Spin-1/2 partlicles only have two possible states ($\uparrow$ & $\downarrow$), they can be elegantly represented in a computer via the bits "1" and "0". More precisely, A lattice state $|S_0^z, S_1^z, \ldots, S_{N-1}\rangle$ is represented as the bit representation of an unsigned integer, with the first bit denoted by the index 0. [7, 59], e.g. $|\uparrow\downarrow\downarrow\uparrow\rangle \hat{=} 1001 \doteq 9$. Symmetries that will come in later, like spin translation or rotation manifest themselves as operations on these bit representations.

1.1.4 Construction of the fixed magnetization basis

A basis list of states having the same magnetization m_z is found by iterating over all integers s from the 2^n dimensional basis and counting the amount of "1" bits $n_\uparrow$, checking whether they amount to the target magnetization $m_z{=}n_\uparrow - N/2$.
With $s[i]$ labeling the i'th bit, starting from 0, the following pseudocode is used to obtain an ordered list of basis states s_a, cf. [7, p. 61] :

$a = 0$
for all $s = 0..2^N - 1$ **do**
  if $\sum_i s[i] = n_\uparrow$ **then**
    $a \leftarrow a + 1$
    $s_a \leftarrow s$
  end if
end for
$M \leftarrow a$

M is the basis dimension. Thus, in terms of M-tuples, a natural basis is given by all vectors

$$\hat{e}_a = (0, \ldots, 0, \underbrace{1}_{c_a}, 0, \ldots, 0)^T, a = 1..M, \tag{1.8}$$

each representing the corresponding integer state s_a.

1.1.5 Construction of the Hamilton matrix

The Hamiltonian (1.2) is translated into a matrix for the fixed magnetization basis cf. [7, p. 60f.]. The diagonal terms are $\langle a|S_i^z S_{i+n}^z|a\rangle = \pm 1/4\ \mu$,since the i'th and $i{+}n$'th spin are either equal or different. The off-diagonal terms $\left(S_i^+ S_{i+n}^- + S_i^- S_{i+n}^+\right)$ flip the bits i and $i{+}n$ $(0 \leftrightarrow 1)$ and amount to zero otherwise. A bisectional search is used to find position b of the flipped state s^*, giving a matrix element contribution of $\langle b|(S_i^+ S_{i+n}^- + S_i^- S_{i+n}^+)|a\rangle = +1/2$. In pseudocode, the matrix belonging to the NNN Hamiltonian $(n = 1, 2)$ is constructed as follows:

for $a = 1..M$ **do**
  for $n = 1, 2$ **do**
    $j = (i + n) \mod N$
    if $a[i] = a[j]$ **then**
      $H(a, a) \leftarrow H(a, a) + \frac{1}{4}\ \mu$

```
        else
            H(a,a) ← H(a,a) − 1/4 μ
            s* = flipstate(a)
            b ← findstate(s*)
            H(a,b) = 1/2
        end if
    end for
end for
```

1.1.6 Diagonalization and time evolution

The Armadillo package [6] is used for matrix diagonalization and vector operations. After setting up the Hamilton matrix, the eigenvectors and eigenvalues are computed. Each eigenstate $|\lambda\rangle$ is a superposition of the natural spin states $|a\rangle = |\uparrow\downarrow\uparrow\uparrow \dots \downarrow\rangle$, which themselves are represented by the bits of an integer. The vectors $\mathbf{c}$, which represent the states and have components c_a, are to be transformed into the eigenbasis. A general initial state $|\psi\rangle$ is decomposed in the eigenbasis as follows:

$$\begin{aligned} H|\psi\rangle &= \sum_a \sum_b |a\rangle \underbrace{\langle a|H|b\rangle}_{H_{ab}} \underbrace{\langle b|\psi\rangle}_{c_b} = \sum_a \sum_b \sum_\lambda |a\rangle \langle a|\lambda|\lambda\rangle \langle\lambda|b\rangle \langle b|\psi\rangle \\ &= \sum_\lambda \lambda |\lambda\rangle \underbrace{\langle\lambda|\psi\rangle}_{c_\lambda}, \end{aligned} \tag{1.9}$$

where c_λ are the components of the vector $\mathbf{c}$ in the eigenbasis and λ are the eigenvalues (energies). The matrix elements and column vectors are what we actually work with. The natural spin states remain untouched.
We would now like to compute the time evolution of the system, which is done in the eigenbasis. Utilizing the time evolution operator $U(t) = e^{-iHt}$ it holds that

$$e^{-iHt}|\psi\rangle = e^{-iHt} \sum_\lambda c_\lambda |\lambda\rangle = \sum_\lambda \underbrace{e^{-i\lambda t} c_\lambda}_{c_\lambda(t)} |\lambda\rangle . \tag{1.10}$$

1.1.7 Measurements and observables

In light of the probabilistic nature of quantum mechanics, we are interested in measuring the expectation value of an observable $\langle O\rangle$. Another important quantity later

on will be the Loschmidt echo M [5], which is generally defined as

$$M(t) = \left|\langle\psi_0|e^{iH_2t}e^{-iH_1t}|\psi_0\rangle\right|. \tag{1.11}$$

For the first test of the time evolution, the special case with $H_2 = 0$ is considered, which makes M a measure of similarity of the time evolved state with the initial state.
The Loschmidt echo is most easily computed in the eigenbasis, since it is not dependent on the basis used, and the eigenbasis is utilized for time evolution anyway. In the matrix picture:

$$\langle\psi_0|e^{-iHt}|\psi_0\rangle = \sum_\lambda \langle\lambda|c_\lambda^* e^{-i\lambda t}c_\lambda|\lambda\rangle = \sum_\lambda c_\lambda^*(0)c_\lambda(t) = \mathbf{c}^*(0)\cdot\mathbf{c}(t). \tag{1.12}$$

For the expectation values of observables, the state vector has to be transformed back into the natural basis because access to the natural spin states is needed in order to evaluate the action of the operators. For example, measurement of $\langle S_i^z\rangle$ is done as follows: For the state vector $\mathbf{c}$ in the natural basis, every state represented by each component like in eq. (1.8) is iterated over and the spin state ($\hat{=}$ bit) of the i'th component of the integer s_a is read out. The expectation value is then

$$\langle S_i^z\rangle_t = \sum_{a,b} c_a^*(t)\,\langle a|S_i^z|b\rangle\,c_a(t) = \sum_a |c_a(t)|^2 S_i^z, \tag{1.13}$$

since the operator S_i^z is diagonal in the natural basis. Analogously, the spin-spin correlation operator $S_i^z S_{i+n}^z$ is handled.

1.2 Tests of the time evolution

We would like to check, whether our time evolution as computed in the previous chapter gives the right results. For this reason, different tests are carried out and compared to theoretical predictions for certain special cases of the dynamics.

1.2.1 Short-time evolution

The goal is to check, whether the computed time evolution is correct up to a small time t. We start from the Heisenberg equation of motion

$$\frac{\mathrm{d}O_H}{\mathrm{d}t} = i[H, O_H], \tag{1.14}$$

where H is the Hamiltonian and

$$O_H(t) = e^{(iHt)} O e^{(-iHt)}. \tag{1.15}$$

The subscript H is dropped in what follows. Using the Baker-Campbell-Hausdorff formula $\mathrm{Ad}_{\exp iHt} = \exp \mathrm{ad}_{iHt}$ and expanding to second order, we get

$$O(t) \approx O + i[H, O]t - \frac{1}{2}\,[H, [H, O]]\, t^2, \quad O \equiv O(0). \tag{1.16}$$

We want to consider the expectation value of the ith spin $\langle S_i^z \rangle$ for the total antiferromagnetic state

$$|a\rangle = |\uparrow\downarrow\uparrow\downarrow \ldots \downarrow\uparrow\downarrow\rangle\,. \tag{1.17}$$

As the Heisenberg equation also holds for expectation values of operators, our expansion reads

$$\langle S_i^z \rangle_t = \langle S_i^z \rangle_0 + i\,\langle [H, S_i^z] \rangle_0\, t - \frac{1}{2}\,\langle [H, [H, S_i^z]] \rangle_0\, t^2 + \mathcal{O}(t^3). \tag{1.18}$$

From eq. (1.4) it is apparent that the linear term drops out, since all angular momentum eigenstates with different S^z are orthogonal to each other. Following the same line of reasoning, and using $S^{\pm} S^{\mp} = \mathbf{S}^2 - (S^z)^2 \pm S^z$, one can show that

$$\begin{aligned} \langle \psi |\, [H, [H, S_i^z]]\, | \psi \rangle &= \langle \psi | \left[(S_{i-1}^+ S_{i-1}^- + S_{i+1}^+ S_{i+1}^-) S_i^z - S_i^+ S_i^- S_{i-1}^z - S_i^+ S_i^- S_{i+1}^z \right] | \psi \rangle \\ &= \langle \psi | \Big[\left(\mathbf{S}_{i-1}^2 - (S_{i-1}^z)^2 + S_{i-1}^z + \mathbf{S}_{i+1}^2 - (S_{i+1}^z)^2 + S_{i+1}^z \right) S_i^z \\ &\qquad - \left(\mathbf{S}_i^2 - (S_i^z)^2 + S_i^z \right) \left(S_{i-1}^z + S_{i+1}^z \right) \Big]\, | \psi \rangle\,. \end{aligned} \tag{1.19}$$

Evaluating this expression for the state given in eq. (1.17) results in the following approximation for the short-time evolution:

$$\langle S_i^z \rangle_t = \pm\frac{1}{2} \mp \frac{1}{2}t^2 + \mathcal{O}(t^3), \tag{1.20}$$

where the upper signs are to be used with a spin up as the initial i state ($|\ldots \underbrace{\uparrow}_{i} \ldots\rangle$) and vice versa. In fig. 1.1, the time evolution of $\langle S_1^z \rangle$ computed with the program is plotted for variable system sizes $N = 2, 4, 6, 8, 10, 12, 14$ with $\mu = 0$, $\lambda = 0$ in eq. (1.2). The dashed blue line is the short-time approximation eq. (1.20), which correctly describes the short-time behaviour of the system. Furthermore, it can be shown that for an infinite system size, the expectation value of the spin can be expressed using the zeroth Bessel function [2, ch. II A]:

$$\langle S_i^z \rangle_t \Big|_{N\to\infty} = \mp\frac{1}{2} J_0(2t), \tag{1.21}$$

which is also shown in fig. 1.1. As N increases, the expectation value computed by the program matches this theoretical prediction longer and longer. Overall, this is a clear indication that the time evolution computed by the program is correct.

1.2.2 Single magnon propagation

The propagation of single or coupled spin flips in the form of "magnons" in a Heisenberg chain is a current area of research. It is interesting to see, whether we can reproduce some of the qualitative findings of other publications. We begin by considering a single spin flip state in a length $N = 31$ chain. The state is given by

$$|a\rangle = |\uparrow\uparrow \ldots \uparrow\uparrow\downarrow\uparrow\uparrow \ldots \uparrow\uparrow\rangle\,. \tag{1.22}$$

In figs. 1.2a to 1.2j, a spacetime matrix plot of the expactation value $\langle S_i^z \rangle_t$ is plotted for $\mu = 0$ and different values of NNN coupling λ. As one can see in fig. 1.2a, for $\lambda = 0$ the single excitation magnon spreads with a well defined velocity of J, which is in agreement to recent studies on the topic, see [4, p. 101]. As confirmed by these studies, the propagation is in no way dependant on the choice of μ. The spin flip in the middle performs a damped oscillation, giving birth to multiple propagation cascades [4, p. 99]. The higher the NNN coupling, the more chaotic the propagation becomes. A particularly interesting feature is seen in fig. 1.2d: A stable region

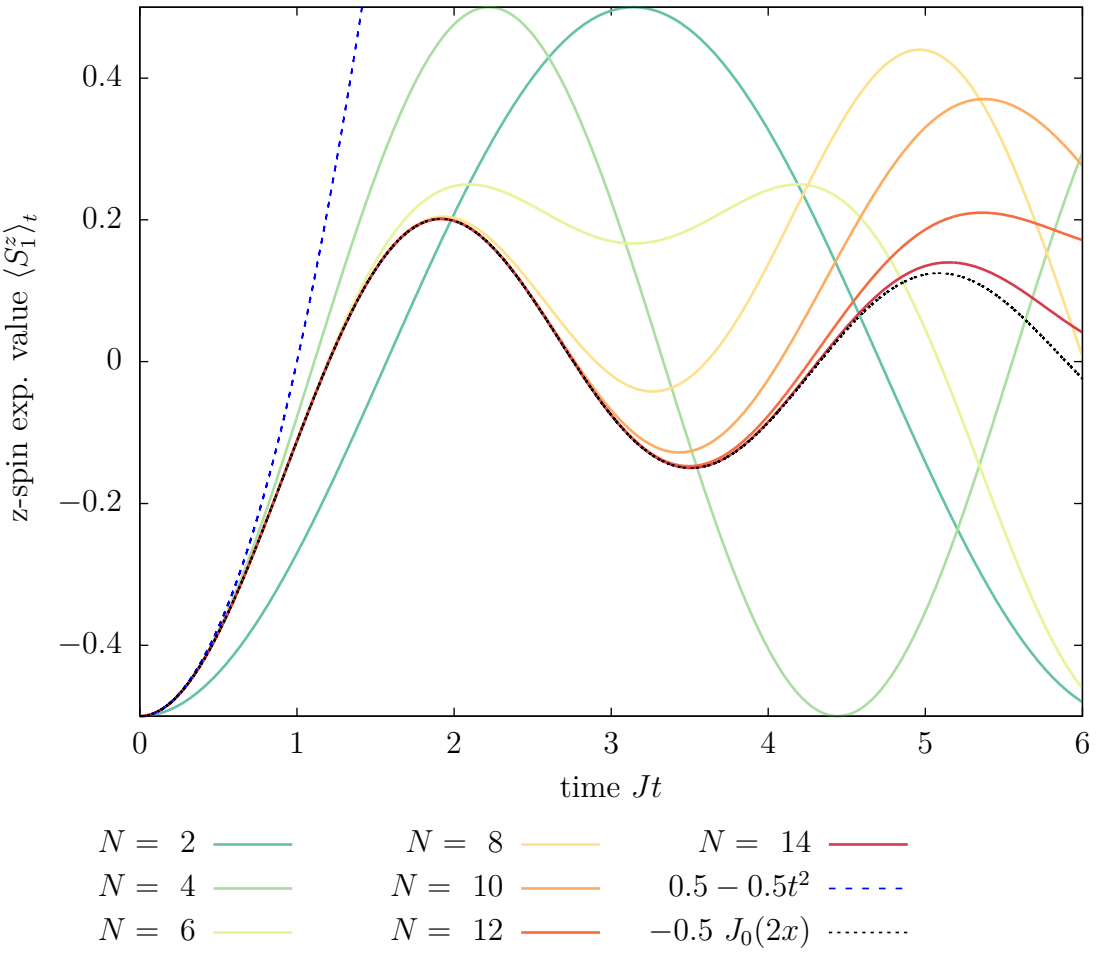

Figure 1.1: In color: Short-time evolution of the expectation value for the first spin of the total antiferromagnetic state eq. (1.17) for different N. In blue-dashed: Short-time approximation calculated by means of a Baker Campbell Hausdorff-expansion. In black-dashed: Theoretical calculation for an infinite-sized system.

with a close to zero expectation value forms in the middle. At even higher λ it also propagates away but stays more or less bound. Note the differences at the boundary in comparison to [4, p. 101], where no periodic boundary conditions were used. Also note that the time axis on the left has been properly scaled to make the different plots comparable. The higher λ, the faster the propagation occurs, which makes sense in the picture that the spin flips get "pulled" by more neighbors. The white peaks are a characteristic of finite systems and arise from magnons traveling in both directions hitting each other and interfering constructively. As this state is similar to the initial state, it corresponds to an echo peak in the Loschmidt echo. As the propagation velocity is J (1 in our case), this peak occurs approximately at $t = JN$.

1.2.3 Multiple-string magnon propagation

This time, we consider a double spin flip in the middle as the initial state:

$$|a\rangle = |\uparrow\uparrow \ldots \uparrow\uparrow\downarrow\downarrow\uparrow\uparrow \ldots \uparrow\uparrow\rangle\,. \tag{1.23}$$

The space time plot for $N = 30$ and $\lambda = 0$ and varying μ is shown in figs. 1.3a to 1.3j. For low μ the qualitative behaviour mirrors that of the previous section. However, when increasing μ, a second, slower propagation cascade is developing and eventually ovepowering the original cascade. This is in agreement to [3] and is explained by the formation of bound states between two spins, so called "two-string magnons". The higher μ, the stronger these spins are bound together and the slower they propagate.

1.2.4 Magnon scattering

When two propagating magnons collide, it can be understood as a scattering event. As [8] outlines, this leads to a displacement. In figs. 1.4a and 1.4b a collision between a two-string magnon and a single magnon are shown. In fig. 1.4a for $\mu = 0$ no displacement can be observed. In fig. 1.4b for $\mu = 5$, there is a clear displacement of the single magnon as it collides with the other: The propagation cascade is shifted to the left, which is in analogy to [8, fig. 5].

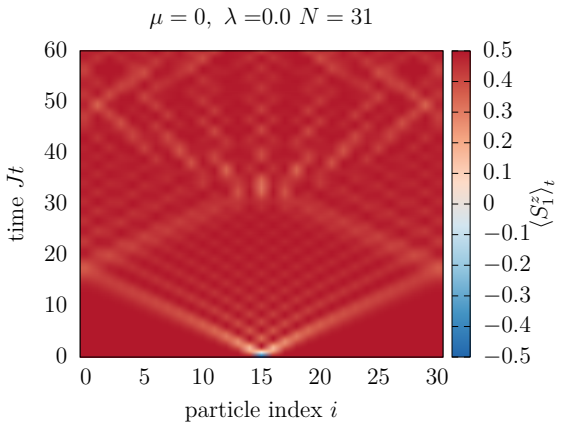

(a) $\lambda = 0$

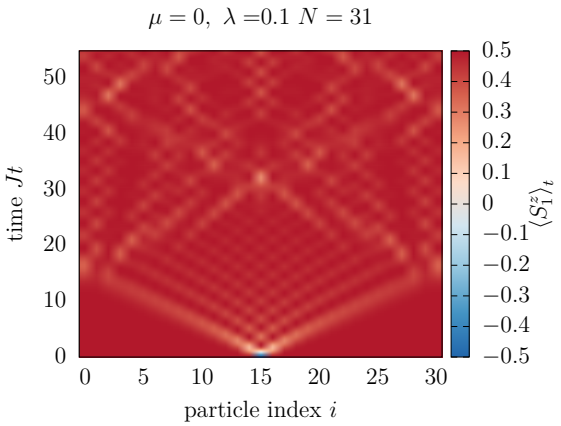

(b) $\lambda = 0.1$

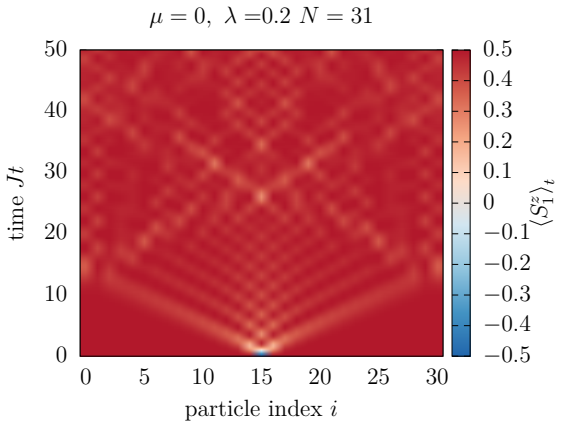

(c) $\lambda = 0.2$

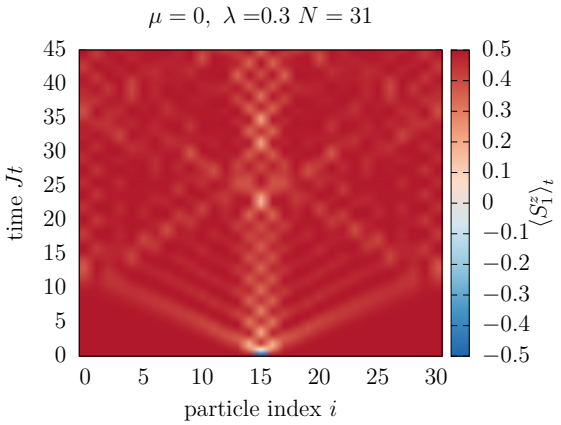

(d) $\lambda = 0.3$

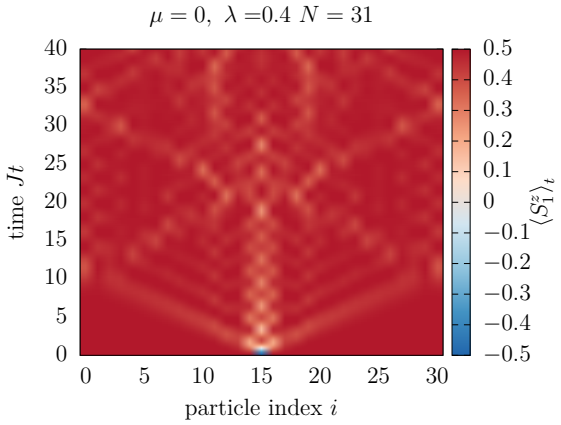

(e) $\lambda = 0.4$

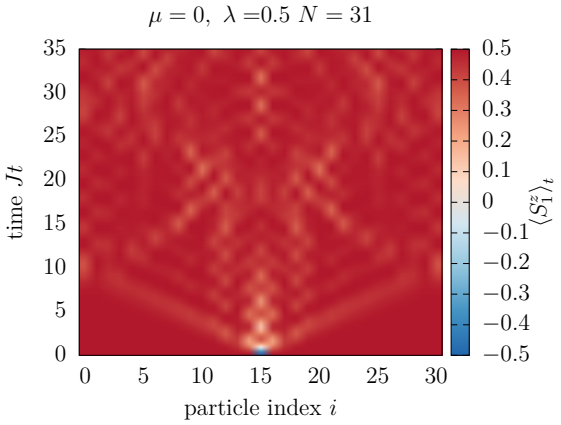

(f) $\lambda = 0.5$

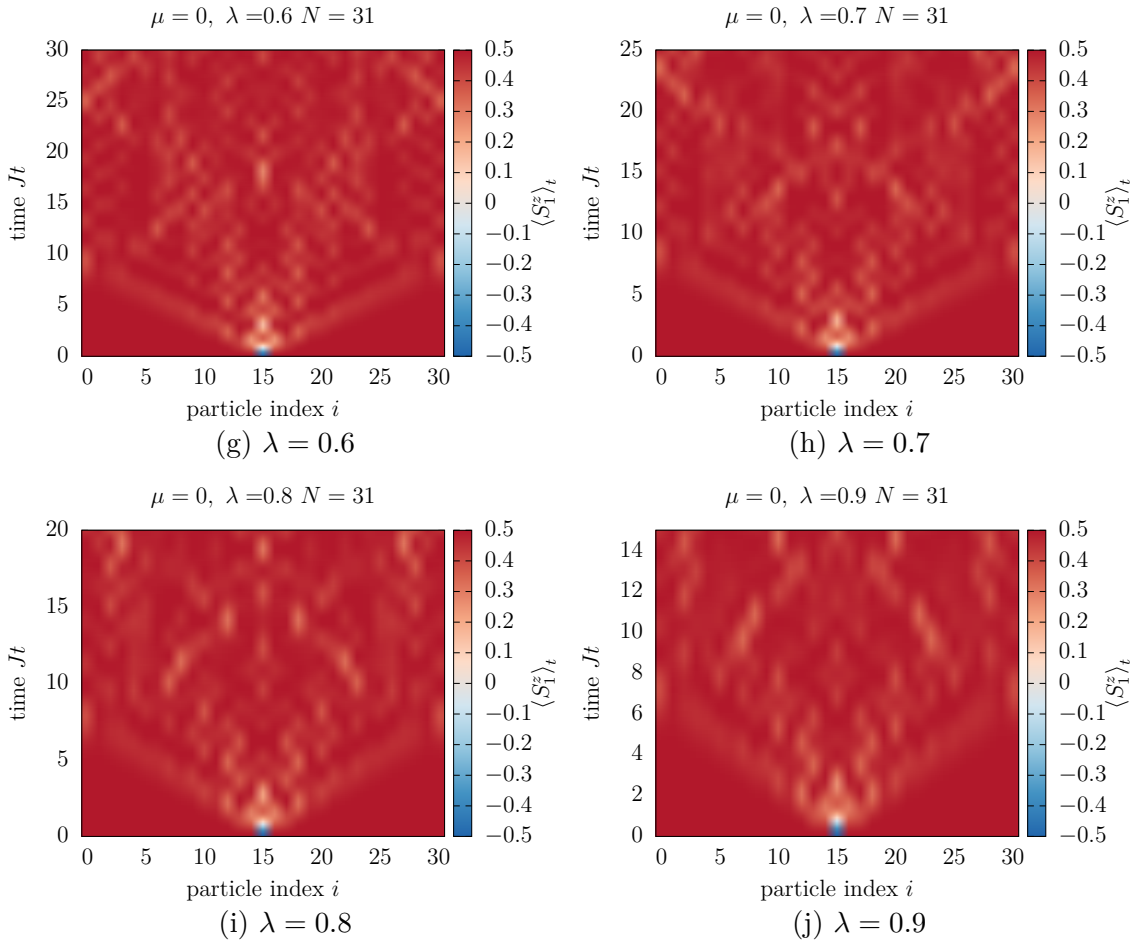

Figure 1.2: Space time plot of the Propagation of single spin excitations in the form of magnons depending on the NNN coupling parameter λ.

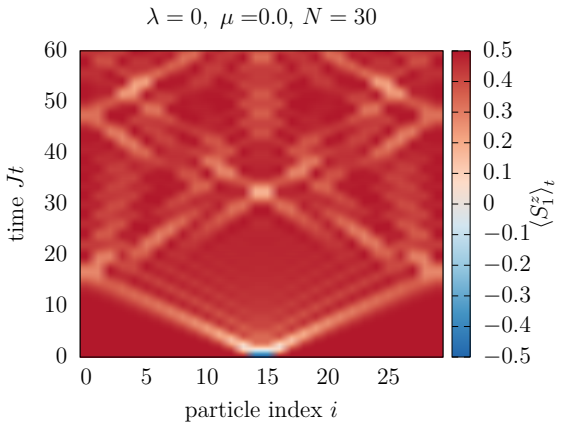

(a) $\mu = 0$

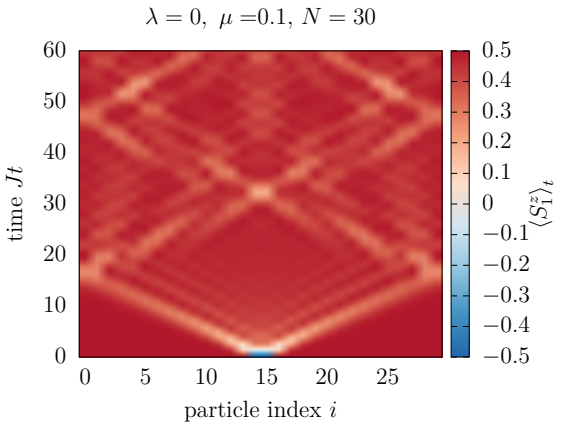

(b) $\mu = 0.1$

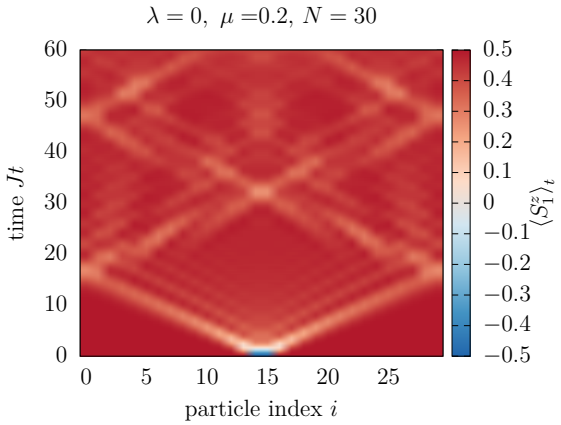

(c) $\mu = 0.2$

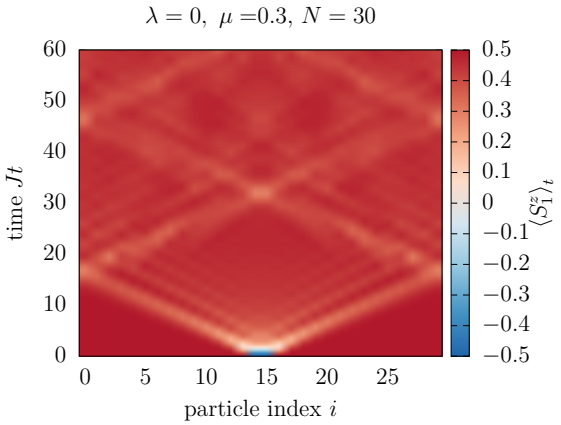

(d) $\mu = 0.3$

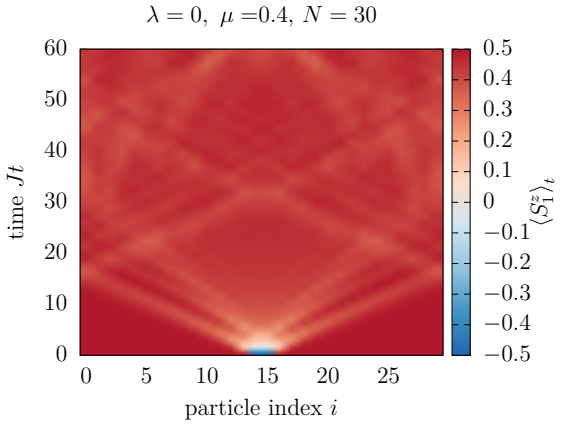

(e) $\mu = 0.4$

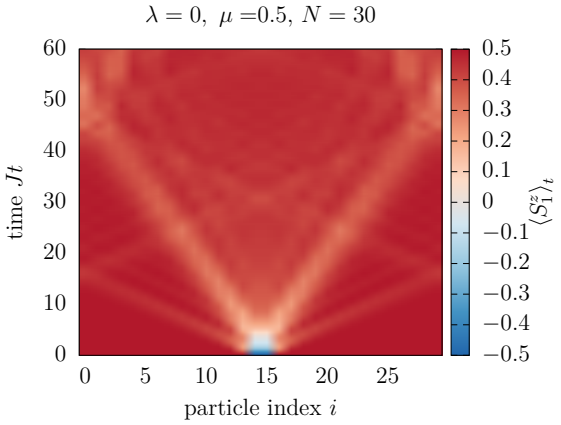

(f) $\mu = 0.5$

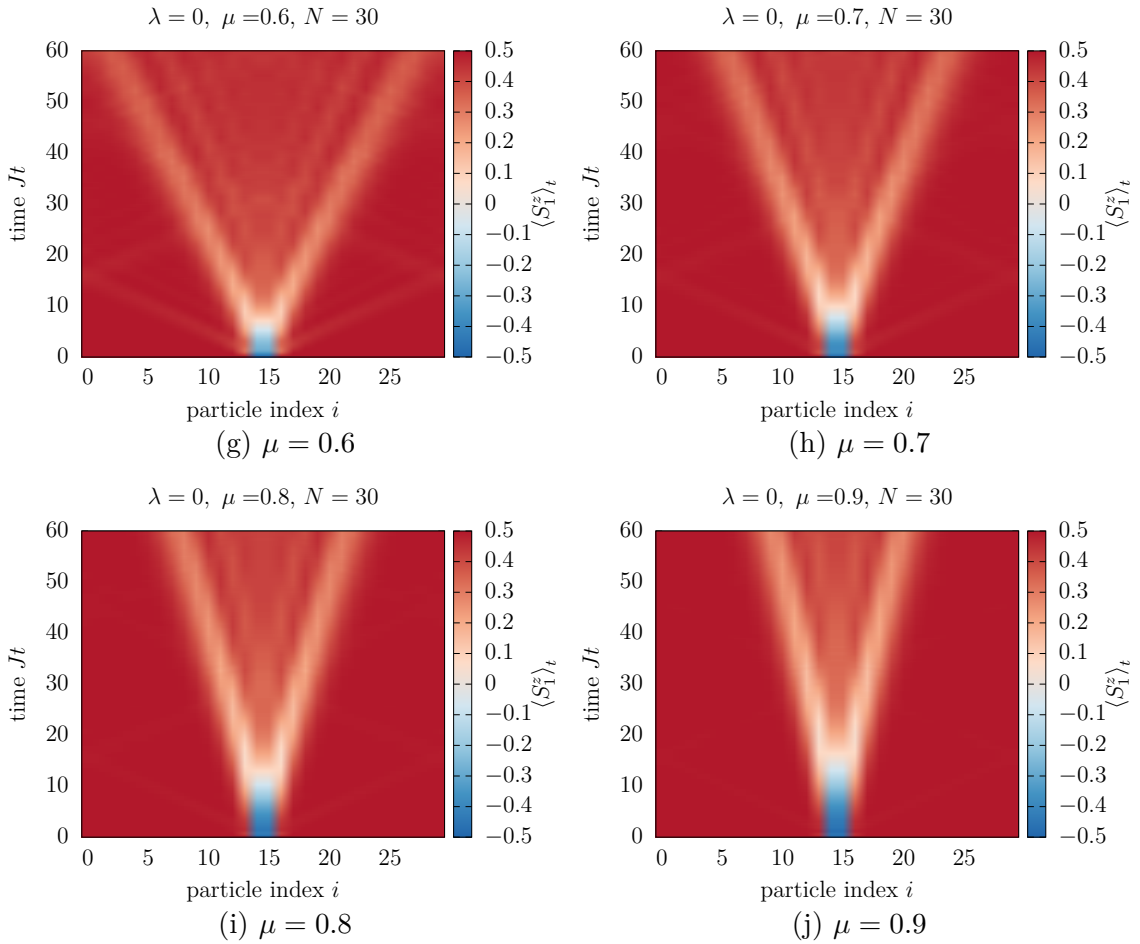

(g) $\mu = 0.6$ (h) $\mu = 0.7$

(i) $\mu = 0.8$ (j) $\mu = 0.9$

Figure 1.3: Two string magnon propagation for $\lambda = 0, N = 30$ for varying μ. For increasing μ, slower propagation cascades coming from bound spins can be observed.

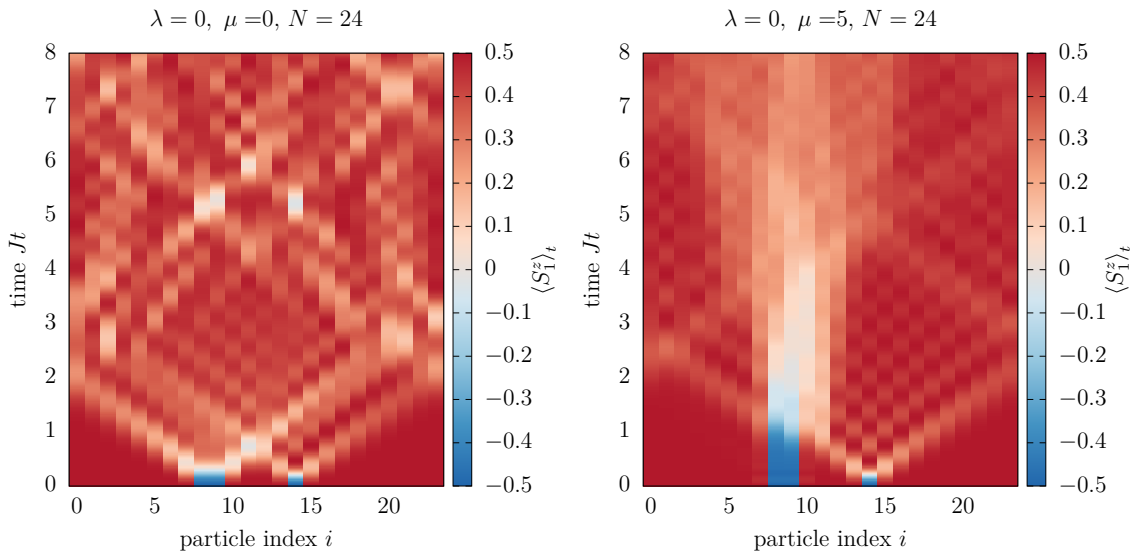

(a) $\mu = 0$ (b) $\mu = 0$

Figure 1.4: Collision of a single magnon with a two-string magnon for $\mu = 0$ and $\mu = 5$. For $\mu = 0$, no displacement is obvserved, whereas for $\mu = 5$, the single magnon is shifted to the left after collision.

1.3 Conclusion

We were able to succesfully implement the Heisenberg XXZ chain in the fixed magnetization basis using a bit representation for the natural states. The system was solved using an exact diagonalization method. The time evolution of the system was tested and verified quantitatively by means of a short-time Baker-Campbell-Hausdorff expansion. Furthermore, qualitative findings from recent publications on the behaviour of single- and two-string magnons have been succesfully reproduced. Additional observables, like the Loschmidt-echo were tested but are not part of this first report. This leaves us with a solid foundation for following studies. Going forward, the focus will be set on the investigetion of time-reversal symmetry-braking, potentially coming about from statistical fluctuations.

Bibliography

[1] *Quantum Magnetism (Lecture Notes in Physics)*. Springer, 2004. ISBN 3540214224.

[2] Peter Barmettler, Matthias Punk, Vladimir Gritsev, Eugene Demler, and Ehud Altman. Quantum quenches in the anisotropic spin- $\frac{1}{2}$ heisenberg chain: different approaches to many-body dynamics far from equilibrium. *New Journal of Physics*, 12(5):055017, 2010. URL `http://stacks.iop.org/1367-2630/12/i=5/a=055017`.

[3] Martin Ganahl, Elias Rabel, Fabian H. L. Essler, and Hans Gerd Evertz. Observing complex bound states in the spin-1/2 heisenberg xxz chain using local quantum quenches. 2011. doi: 10.1103/PhysRevLett.108.077206.

[4] Martin Jakob Ganahl. Simulation of spin transport in one dimensional quantum heisenberg 1/2 systems in real time. Master's thesis, Graz University of Technology, 2010.

[5] A. Goussev, R. A. Jalabert, H. M. Pastawski, and D. Ariel Wisniacki. Loschmidt echo. *Scholarpedia*, 7(8):11687, 2012. revision 127578.

[6] Conrad Sanderson. Armadillo: An Open Source C++ Linear Algebra Library for Fast Prototyping and Computationally Intensive Experiments. Technical report, NICTA, September 2010.

[7] Anders W. Sandvik. Computational Studies of Quantum Spin Systems. *AIP Conf. Proc.*, 1297:135, 2010. doi: 10.1063/1.3518900.

[8] Rogier Vlijm, Martin Ganahl, Davide Fioretto, Michael Brockmann, Masudul Haque, Hans Gerd Evertz, and Jean-SÃ©bastien Caux. Quasi-soliton scattering in quantum spin chains. 2015. doi: 10.1103/PhysRevB.92.214427.